SMOOTHING EFFECTS OF ANTENNA APERTURE ON VARIANCE AND SPECTRUM OF AMPLITUDE SCINTILLATION AT Ka-BAND

Christian Ho
Jet Propulsion Laboratory, California Institute of Technology, Pasadena, CA, USA
E-mail: Christian.ho@jpl.nasa.gov

1. Introduction: The Earth's atmosphere and weather have much larger degradation effects on Ka-band than other lower frequency bands. Fast amplitude variations due to atmospheric scintillation are the main concerns for Deep Space Network (DSN) Ka-band downlink under clear weather conditions. Fast amplitude fluctuations (< min) or fading slopes will directly affect the times of loss of lock and recovery and short-term dynamics of the systems.

Higher data rates imply a new sensitivity to short term amplitude fluctuations. When the wavelength of Ka-band radio waves is comparable to the Fresnel length of the atmospheric turbulences, fast scintillations (0.1-10 Hz) become significant. Receiving signals appear highly dynamic at their amplitude and phase. These fast variations on amplitude and phase of signals are different from those slow variations caused by rain or cloud attenuations. Fast variations often superimpose on top of slow fading, causing deep fading in a short time. The temporal spectrum of amplitude scintillation is dependent on frequency of microwave signals (or wavelength), wind speed, Fresnel length of turbulent eddy zone, and antenna aperture [1,2,3,4].

However, a detailed investigation for large antenna at Ka-band has never been done due to the lack of experiments and applications in the past. We need to understand severity of amplitude variances and frequency range of fast fluctuations at Ka-band for a finite aperture receiver. In this paper, we will study how much amplitude variances can be reduced due to the aperture smoothing effects for a large antenna such as a DSN station. Scaling factors on signal frequency, antenna size, and elevation angle will also be theoretically investigated.

2. Solutions for a point receiver (a_r = 0): Considering a vertically downward propagating microwave, as shown in Figure 1, after encountering a turbulent eddy, the signal will be diffracted with a small angle θ (weak scattering). The solution of amplitude variance for a point receiver is:

$$\left\langle \chi^2 \right\rangle = 4\pi^2 k^2 \int_0^\infty \kappa d\kappa \Phi_n(\kappa) \int_0^\infty \sin(\frac{z\kappa^2}{2k}) dz \qquad (1)$$

After applying the Kolmogorov turbulent spectrum: $\Phi_n(\kappa) = 0.033 C_n^2(z)\kappa^{-11/3}$, for a slab model with thickness H, $\left\langle \chi^2 \right\rangle = 0.307 C_n^2 H^{11/6} k^{7/6} (Np)^2$; for a thin layer model with thickness ΔH, $\left\langle \chi^2 \right\rangle = 0.563 C_n^2 \Delta H H^{5/6} k^{7/6} (Np)^2$. When we extend equation (1) to an exponential model with scale height H, the solution is $\left\langle \chi^2 \right\rangle = 0.530 C_n^2 H^{11/6} k^{7/6} (Np)^2$ where $\langle \chi \rangle (dB) = 4.34 \langle \chi \rangle (Np)$.

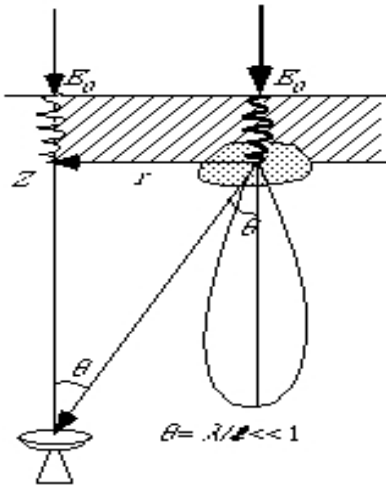

Figure 1. A geometry showing how a microwave passing through a turbulent refractivity eddy is refracted to a receiver with a small angle.

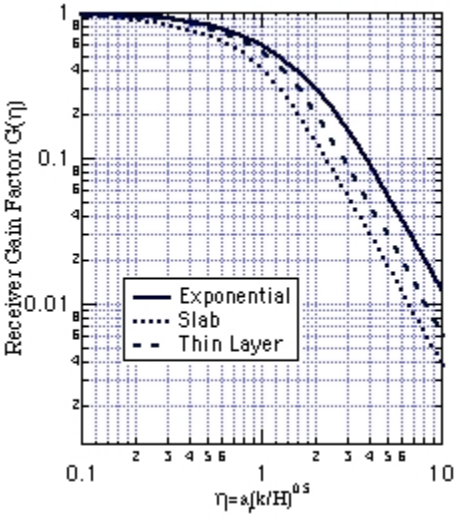

Figure 2. Gain factors for three types of turbulent layer models as a function of antenna radius a_r. The exponential model has larger gain factor among three models.

ISBN: 4-88552-207-2 C3055©IEICE

Under Taylor's frozen field assumption, the temporal covariance can be converted into the spatial covariance. The power spectrum for a point receiver is

$$W_\chi(\omega) = \int_{-\infty}^{\infty} C_\chi(\tau) e^{i\omega\tau} d\tau = 4\pi^2 H k^2 \int_{\omega/\upsilon}^{\infty} d\kappa \kappa \Phi_n(\kappa) \frac{1}{\sqrt{\kappa^2\upsilon^2 - \omega^2}} (1 - \frac{\sin(\kappa^2 H/k)}{\kappa^2 H/k}) \tag{2}$$

For a slab turbulent model, we have

$$W_\chi(\omega) = 1.096 \frac{HC_n^2 k^2 \upsilon^{5/3}}{\omega^{8/3}} \left\{ 1 - \frac{0.594\omega_0^2}{\omega^2} I_m \left[\exp(i\frac{\omega^2}{\omega_0^2}) \Gamma(\frac{1}{2}) U(\frac{1}{2}, -\frac{4}{3}, i\frac{\omega^2}{\omega_0^2}) \right] \right\} \tag{3}$$

where U is the first solution of the Kummer function. After taking low and high frequency approximations, we have

$W_\chi^\infty(\omega) = 1.096 \frac{HC_n^2 k^2 \upsilon^{5/3}}{\omega^{8/3}} (Np)^2/Hz \quad \omega >> \omega_0$, while $W_\chi^0(\omega) = 0.425 \frac{H^{7/3} k^{2/3} C_n^2}{\upsilon} Np)^2/H \quad for \quad \omega = 0$

The normalized ratio: $\frac{W_\chi(\omega)}{W_\chi(0)} = 2.577 (\frac{\omega_0}{\omega})^{8/3} \left\{ 1 - \frac{0.594\omega_0^2}{\omega^2} I_m \left[\exp(i\frac{\omega^2}{\omega_0^2}) \Gamma(\frac{1}{2}) U(\frac{1}{2}, -\frac{4}{3}, i\frac{\omega^2}{\omega_0^2}) \right] \right\}$ (4)

where, we have defined $\omega_0 = \upsilon\sqrt{k/H} = \upsilon/\sqrt{\lambda H/2\pi} = \upsilon/l_0$ (wind speed over the Fresnel length) as the Fresnel frequency which is the most important parameter in governing the scintillation fluctuations, because only the eddies with Fresnel length l_0 are most efficient in generating the amplitude scintillations. We also define the corner frequency ω_c as the intersection between the asymptotes for high frequency and low frequency, which will define the shape of power spectrum. The calculation shows $\omega_c = 1.43\omega_0$ for a slab model; $\omega_c = 1.04\omega_0$ for a thin layer model [3,4]; and $\omega_c = 0.97\omega_0$ for an exponential model.

3. Solutions for a finite aperture receiver ($a_r \neq 0$): For a receiver with finite aperture antenna, the amplitude variance is: $\overline{\langle \chi^2 \rangle} = 4\pi^2 k^2 \int_0^\infty \kappa d\kappa \Phi_n(\kappa) \int_0^\infty \sin(z\kappa^2/2k) [2J_1(\kappa a_r)/\kappa a_r]^2 dz$ (5)

For a slab model with thickness H, $\langle \chi^2 \rangle = 0.307 C_n^2 H^{11/6} k^{7/6} G_1(a_r\sqrt{2\pi/\lambda H})(Np)^2$, where $G(\eta)$ is the gain factor function for the aperture averaging effect. For a thin layer model with thickness H, $\langle \chi^2 \rangle = 0.563 C_n^2 \Delta H H^{5/6} k^{7/6} G_2(a_r\sqrt{2\pi/\lambda H})(Np)^2$. Also when we extend equation (5) into an exponential model with thickness H, the solution is $\langle \chi^2 \rangle = 0.530 C_n^2 H^{11/6} k^{7/6} G_3(a_r\sqrt{2\pi/\lambda H})(Np)^2$.

Amplitude variances are estimated for an oblique earth-space path as a function of elevation angle using $H/\sin\theta$ to replace H in above equations. Gain factors $G(\eta)$ as a function of antenna radius (a_r) for three turbulent models are shown in Figure 2. The elevation angle dependence of amplitude change (in dB) for both types of receivers is shown in Figure 3. The dependence of wavelength ($\lambda = 2\pi/k$) and antenna size can be found from above equations and Figure 2.

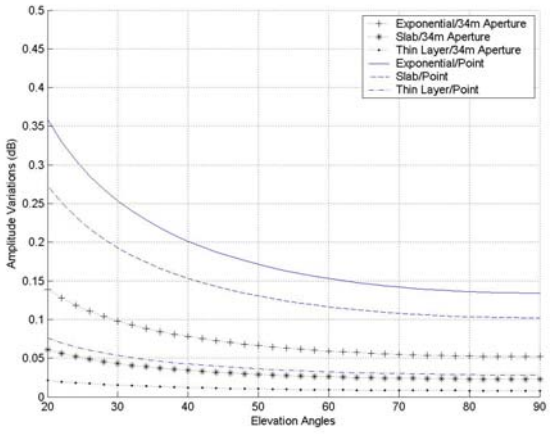

Figure 3. Elevation angle dependence of amplitude variations (in dB) for both of a 34m DSN antenna and a point receiver for three types of atmospheric turbulent models.

The power spectrum for a finite aperture receiver is a convolution of the spectral fluctuations with a two-dimensional antenna with a circular surface [2,5]:

$$W_{\bar{\chi}}(\omega,a_r)=4\pi^2Hk^2\int_{\omega/\upsilon}^{\infty}d\kappa\kappa\Phi_n(\kappa)\frac{1}{\sqrt{\kappa^2\upsilon^2-\omega^2}}(1-\frac{\sin(\kappa^2H/k)}{\kappa^2H/k})\left[\frac{2J_1(\kappa a_r)}{\kappa a_r}\right]^2 \quad (6)$$

Using a Gaussian pattern $\exp(-b^2\kappa^2a_r^2)$ to approximate $[2J_1(\kappa a_r)/\kappa a_r]^2$ [3], where the best fit is b=0.4832, we can analytically solve the above equation. The solution is

$$W_{\bar{\chi}}(\omega,a_r)=\frac{0.652Hk^2C_n^2}{\omega}\left(\frac{\upsilon}{\omega}\right)^{5/3}\left\{\Gamma(\frac{1}{2})U(\frac{1}{2},-\frac{1}{3},\frac{\omega^2}{\omega_s^2})\exp(-\frac{\omega^2}{\omega_s^2})-(\frac{\omega_0}{\omega})^2I_m\left[\Gamma(\frac{1}{2})U(\frac{1}{2},-\frac{4}{3},\frac{\omega^2}{\omega_s^2}-i\frac{\omega^2}{\omega_0^2})\exp(-\frac{\omega^2}{\omega_s^2}+i\frac{\omega^2}{\omega_0^2})\right]\right\}$$

here we have defined a frequency called as the aperture smoothing frequency $\omega_s=\upsilon/ba_r$ which is the frequency of wind speed over the entire antenna area. It is equivalent that an antenna with finite aperture imposes a high wave number cutoff on the spectrum of the refractivity fluctuations (similar to a low-pass filter). After a high frequency approximation, the above solution becomes

$$W_{\bar{\chi}}^{\infty}(\omega,a_r)=1.155Hk^2C_n^2\upsilon^{5/3}\omega^{-8/3}(\omega_s/\omega)\exp(-\omega^2/\omega_s^2) \quad (7)$$

Thus, the normalized ratio is $W_{\bar{\chi}}^{\infty}(\omega,a_r)/W_{\chi}^{\infty}(\omega,0)=1.053(\omega_s/\omega)\exp(-\omega^2/\omega_s^2)$. The low frequency approximation results in $W_{\bar{\chi}}^{0}(\omega,a_r)=0.6515H^{7/3}k^{2/3}C_n^2\upsilon^{-1}\left\{\Gamma(-4/3)(\omega_s^2/\omega_0^2)^{4/3}-I_m\left[\Gamma(-7/3)(\omega_s^2/\omega_0^2-i)^{7/3}\right]\right\}$. Its normalized ratio is $W_{\bar{\chi}}^{0}(\omega,a_r)/W_{\chi}^{0}(\omega,0)=1.533\left\{\Gamma(-4/3)(\omega_s^2/\omega_0^2)^{4/3}-I_m\left[\Gamma(-7/3)(\omega_s^2/\omega_0^2-i)^{7/3}\right]\right\}$. These spectral solutions and ratios are shown in Figures 4 and 5 for a case of $\omega_s=0.68\omega_0$ (equivalent to a 34m antenna). The cross-normalized ratio which defines the corner frequency for a finite aperture receiver is shown in equation (8). It can only be solved graphically as marked in Figures 4 and 5.

$$W_{\bar{\chi}}^{\infty}(\omega,a_r)/W_{\bar{\chi}}^{0}(\omega,a_r)=1.773(\omega_0/\omega)^{8/3}(\omega_s/\omega)\exp(-\omega^2/\omega_s^2)\left\{\Gamma(-4/3)(\omega_s^2/\omega_0^2)^{4/3}-I_m\left[\Gamma(-7/3)(\omega_s^2/\omega_0^2-i)^{7/3}\right]\right\}^{-1} \quad (8)$$

We can see that the high frequency spectrum for a finite aperture receiver significantly deviates from that for a point receiver. It damps off at a rate much faster than the power law of -8/3 for a point receiver. The aperture smoothing frequency as a function of antenna aperture size is shown in Figure 6, while the corner frequency as a function of aperture smoothing frequency is shown in Figure 7.

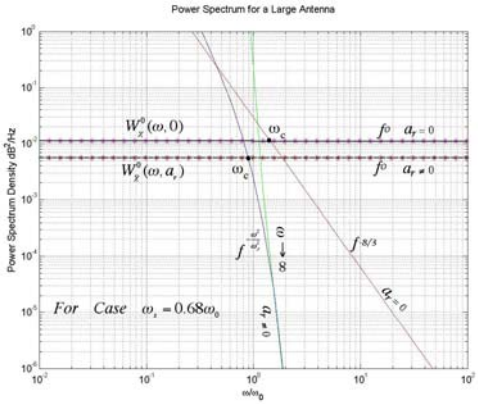

Figure 4. Power spectrum density (dB²/Hz) as a function of ω/ω_0 for a case of $\omega_s=0.68\omega_0$.

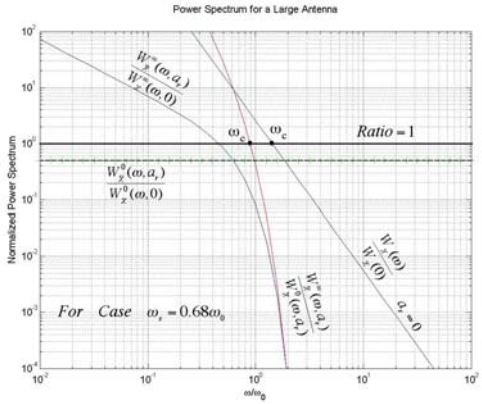

Figure 5. Normalized power spectrum density as a function of ω/ω_0 for a case of $\omega_s=0.68\omega_0$.

4. Applying to a DSN station: Now we can apply these analytic solutions to a 34-m (diameter) parabolic dish antenna at the Goldstone DSN site at Ka-band [6]. We will use the following parameters for the Goldstone site calculation: $C_n^2=0.5\times10^{-13}(m^{-2/3})$, $\lambda=0.01(m)$, $H=9.5\times10^3(m)$, $a_r=34/2\times70\%(m)$, and $\upsilon=10(m/s)$. Here we have assumed that the dish antenna has a 70% efficiency. For an exponential turbulent layer, when $\eta=a_r\sqrt{2\pi/\lambda H}=3.06$, the gain factor $G(\eta)=0.15$. Thus, when elevation angle $\theta=$ 90°, $\langle\chi^2\rangle=1.43\times10^{-4}(Np)^2$ and its root of mean square (rms) $\chi=0.012(Np)=0.052(dB)$. When $\theta=$ 20°, $\langle\chi^2\rangle=1.02\times10^{-3}(Np)^2$ and its root of mean square (rms) $\chi=0.032(Np)=0.140(dB)$. The Fresnel frequency $\omega_0=\upsilon/\sqrt{\lambda H/2\pi}=2.6(Radian/s)$ and $f_0=0.41Hz$. The aperture smoothing frequency $\omega_s=\upsilon/ba_r=1.74(Radian/s)$, $f_s=0.27Hz$, and $\omega_s=0.68\omega_0$. The corner frequency: $\omega_c=2.34(radian/s)=0.9\omega_0$ and $f_c=0.38Hz$. If we define the fading rate (or fading slope) by $r_f=\delta_\chi\cdot f_c$, where δ_χ is the maximum rms of amplitude variance (or amplitude changes in dB), we have the maximum fading rate $r_f=0.14(dB)\times0.38(Hz)\approx0.05dB/s$. For a 70m diameter receiver, we have

$\omega_s = 0.33\omega_0$ and $\omega_c = 0.50\omega_0$. The corner frequency reduces to 0.2Hz, nearly two times less than that for a 34m antenna. Above the corner frequency $\omega_c = 1.43\omega_0$ the power spectrum damps at a rate of $f^{-8/3}$ for a point receiver, and above $\omega_c = 0.9\omega_0$ it rolls off at a rate of $f^{-\omega^2/\omega_s^2}$ for a 34m diameter receiver, respectively.

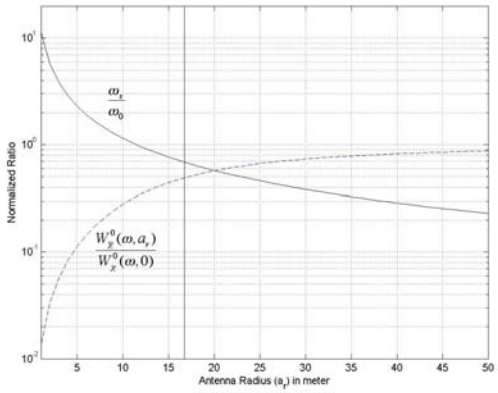

Figure 6. The ratio of ω_s / ω_0 as a function of antenna aperture radius a_r. A normalized low frequency approximation of $W_\chi^0(\omega, a_r)$ is also shown. A vertical line at a_r = 17m shows cross values for two curves.

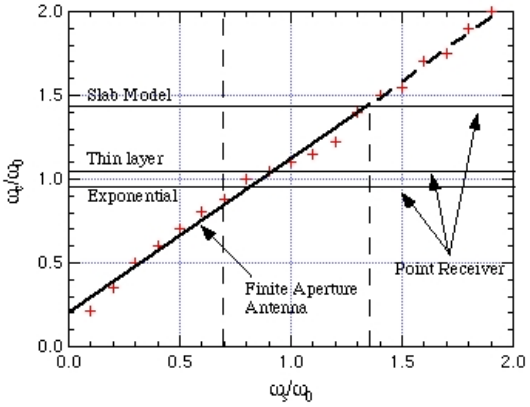

Figure 7. Normalized corner frequency ω_c / ω_0 as a function on the ratio of ω_s / ω_0. The upper limit of the corner frequency ω_c for both point receivers and finite aperture receivers is 1.43 ω_0.

5. Summary: A theoretical study of variances of amplitude scintillations and power spectrum for a finite aperture antenna has been performed. Amplitude variances for a weak scattering scenario are studied using the turbulence theory. At first, the Kolmogorov turbulent spectrum is applied into a point receiver for three types of turbulent layer models, especially for an exponential model varying with altitude. Then the analytic solutions are extended to a receiver with a finite aperture antenna for three types of turbulent models through a two dimensional integration over the antenna surface. Smoothing effects of antenna aperture are investigated through gain factor expressions. Scintillation power spectrum solutions are analytically derived for both a point receiver and a finite aperture receiver. The aperture smoothing frequency (ω_s), corner frequency (ω_c), and dumping rate are introduced to define the shape of spectrum for a finite aperture antenna. The emphasis has been put on quantitatively describing the aperture smoothing effects and graphically solving the corner frequency for a large aperture receiver. Power spectral shapes are parametrically analyzed in detail through both low and high frequency approximations. It is found that averaging effects become significant when the transverse correlation length of the scintillation is smaller than the antenna radius. The upper frequency (corner frequency) for a finite aperture receiver is controlled by both the Fresnel frequency and aperture smoothing frequency. Above the coner frequency, the spectrum rolls off at a much faster rate of $f^{-\omega^2/\omega_s^2}$ instead a rate of $f^{-8/3}$ as for a point receiver. We have applied these solutions into the scenario of a DSN Goldstone 34m antenna. Scintillation intensity for amplitude changes is estimated and the power spectrum shape is predicted for the receiving station. We find that at 20° elevation angle, the amplitude change (rms) is 0.14 dB, while at 90° the change is 0.05 dB for the 34m diameter antenna. The maximum corner frequency for the receive is found to be 0.38 Hz (or 0.9 ω_0), while the fading rate (or fading slope) is 0.05 dB/s. These results will aid us in telecom system design, Ka-band experimental sample rate selection, and extrapolation of the Ka-band fading models developed from previous ACTS and Olympus experiments [7,8,9] in use for a large receiving station such as the DSN. It also provides the theoretical basis for further comparison with any experimental measurements at Ka-band.

Acknowledgements: The author wishes to thank Dr. Albert Wheelon for his consulting work on this study. He is also indebted to the help from Dr. Charles Lee and Kelly Gritton in computing work.

References: [1] Wheelon, A.D., *Electromagnetic Scintillation II. Weak Scattering*, 2003. [2] Tatarski, V.I., *The Effects of the Turbulent Atmosphere on Wave Propagation*, 1971. [3] Haddon, J. and E.Vilar, *IEEE Trans. Antennas Propagat.*, vol. AP-34, No.5, 646, 1986. [4] Moulsley, T.J., and E. Vilar, *IEEE Trans. Antennas Propagat.*, vol. AP-30, No. 6, 1099, 1982. [5] Wheelon, A.D., *J. Appl. Phys.*, vol. 28, no. 6, 684, 1957. [6] Linfield, R., *JPL TDA Progress Report*, 42-124, February 15, 1996. [7] Crane, R.K.,et al., *Proc. IEEE*, 85(6), 936, 1997. [8] Otung, I.E., et al., *IEEE Trans. Antennas Propagat.*, vol. AP-46, No. 10, 1580, 1998. [9] Cox, D.C., et al., *Radio Sci.*, vol, 16, no. 5, 885, 1981.